

## Supplementary Information for

### A peptide toxin in ant venom mimics vertebrate EGF-like hormones to cause long-lasting hypersensitivity in mammals

David A. Eagles,<sup>1</sup> Natalie J. Saez,<sup>1,2</sup> Bankala Krishnarjuna,<sup>3</sup> Julia J. Bradford,<sup>4</sup> Yanni K.-Y. Chin,<sup>1</sup> Hana Starobova,<sup>1</sup> Alexander Mueller,<sup>1</sup> Melissa E. Reichelt,<sup>4</sup> Eivind A.B. Undheim,<sup>5,6</sup> Raymond S. Norton,<sup>3,7</sup> Walter G. Thomas,<sup>4</sup> Irina Vetter,<sup>1,8</sup> Glenn F. King<sup>1,2</sup> and Samuel D. Robinson<sup>1,\*</sup>

<sup>1</sup>Institute for Molecular Bioscience, The University of Queensland, Brisbane, QLD 4072, Australia  
<sup>2</sup>Australian Research Council Centre of Excellence for Innovations in Peptide and Protein Science, The University of Queensland, QLD 4072, Australia

<sup>3</sup>Monash Institute of Pharmaceutical Sciences, Monash University, Melbourne, VIC 3052, Australia  
<sup>4</sup>School of Biomedical Sciences, The University of Queensland, Brisbane, QLD 4072, Australia

<sup>5</sup>Centre for Biodiversity Dynamics, Department of Biology, NTNU, N-7491 Trondheim, Norway

<sup>6</sup>Centre for Ecological and Evolutionary Synthesis, Department of Biosciences, University of Oslo, 0316 Oslo, Norway

<sup>7</sup>Australian Research Council Centre for Fragment-Based Design, Monash University, Parkville, Victoria 3052, Australia

<sup>8</sup>School of Pharmacy, The University of Queensland, Brisbane, QLD 4102, Australia

\*Corresponding author: Samuel D. Robinson (S.D.R.)

**Email:** sam.robinson@uq.edu.au

#### **This PDF file includes:**

Figures S1 to S7  
Table S1

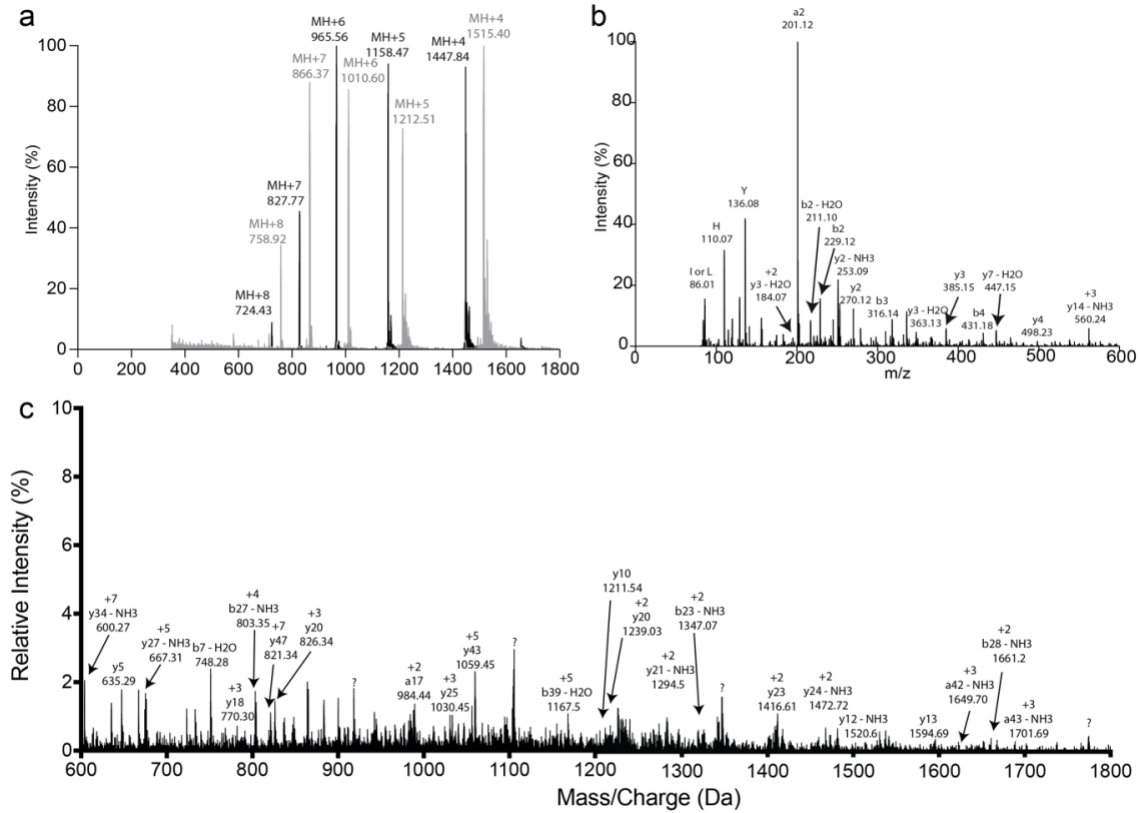


**Fig. S1. MS analysis of the RP-HPLC fraction corresponding to Mg1a.** (a) MS of Mg1a fraction (observed monoisotopic  $MH^{+6}$  965.56 m/z; theoretical monoisotopic mass  $MH^{+6}$  965.57 m/z). Reduction and alkylation of the fraction produced a mass shift indicative of the presence of three intrachain disulfide bonds (observed monoisotopic  $MH^{+6}$  1010.60 m/z; theoretical monoisotopic  $MH^{+6}$  1010.60 m/z). (b,c) MS/MS spectrum of reduced and alkylated Mg1a fraction.

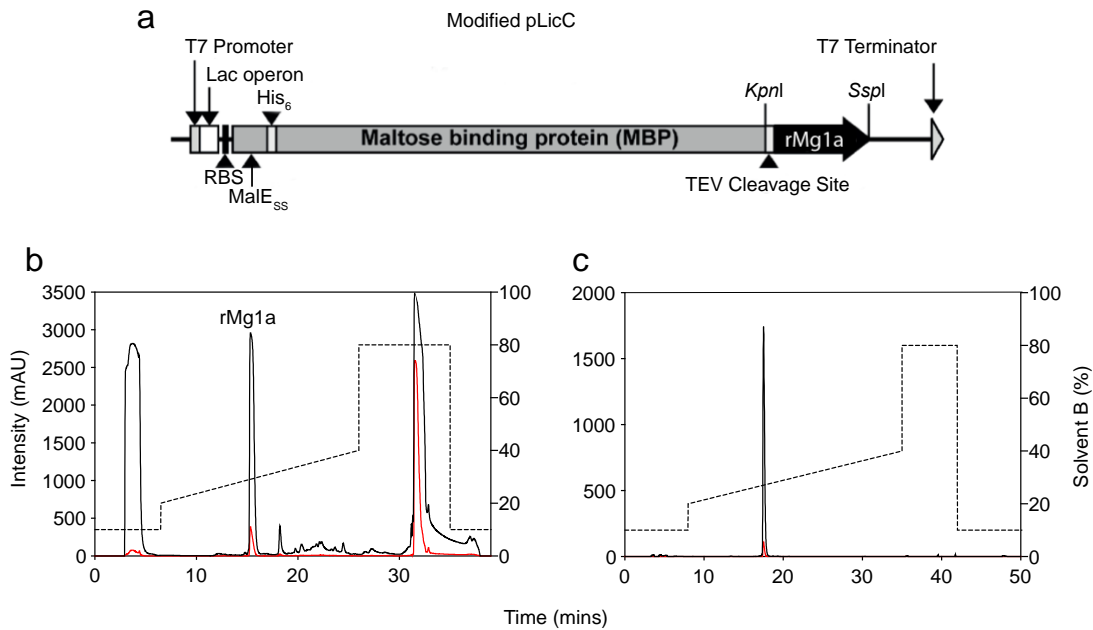


**Fig. S2. Figure S2. Expression and purification of rMg1a.** (a) Schematic of rMg1a pLIC plasmid vector. The vector utilizes a T7 RNA polymerase promoter, an inducible lac operon allowing for controlled expression of the target gene, a ribosome binding site (RBS), MalE signal sequence for periplasmic export, a His<sub>6</sub> tag for nickel affinity purification, maltose binding protein (MBP) to enhance fusion protein solubility, a tobacco etch virus (TEV) recognition site to allow for TEV protease cleavage of the fusion protein, and finally restriction enzyme sites (*KpnI*, *SspI*) to allow for insertion of the Mg1a gene into the vector. (b) RP-HPLC chromatogram of *E. coli* soluble cell lysate following nickel affinity chromatography and TEV protease cleavage. Cleavage products were eluted on a C18 semi-preparative RP-HPLC column using a 20–40% gradient of solvent B (90% ACN, 0.043% TFA) over 30 min. (c) rMg1a obtained from the semi-preparative RP-HPLC purification (shown in (b)) was analysed by C18 analytical RP-HPLC to assess the purity of the recombinant peptide. Black and red traces in panels a and b represent absorbance at 214 nm and 280 nm, respectively, while the dotted lines indicate the percentage of solvent B. The final yield of purified peptide was 1.8 mg/L culture.

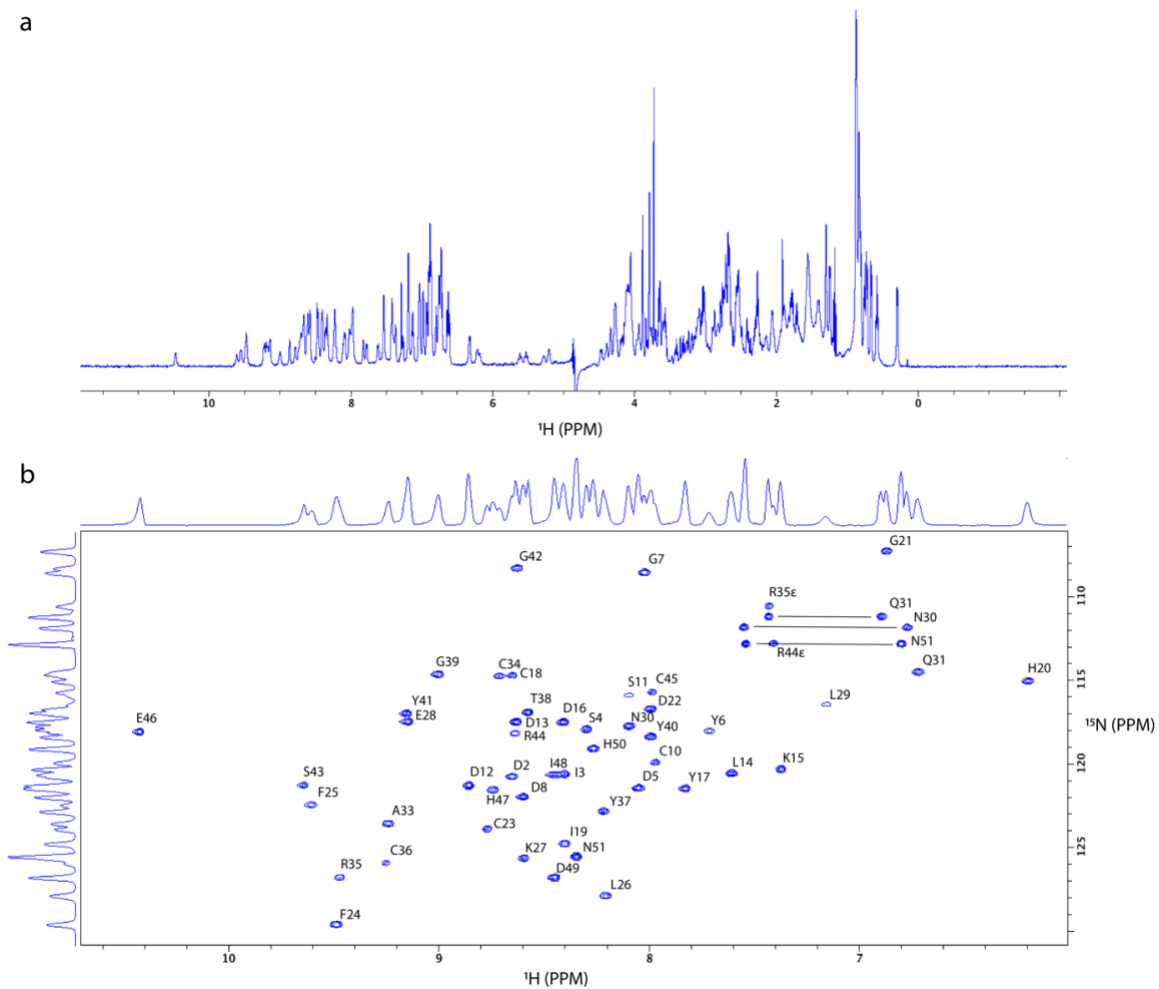


**Figure S3. rMg1a adopts a single major conformation and is highly structured in solution.** (a) 1D  $^1\text{H}$  NMR spectrum of rMg1a. (b) 2D [ $^1\text{H}$ - $^{15}\text{N}$ ]-HSQC spectrum of  $^{15}\text{N}$ -labelled rMg1a. Spectra were acquired at 20°C on a Bruker Avance III 600 MHz spectrometer, using a 350  $\mu\text{M}$  sample of rMg1a at pH 6.0 in 20 mM sodium phosphate buffer.

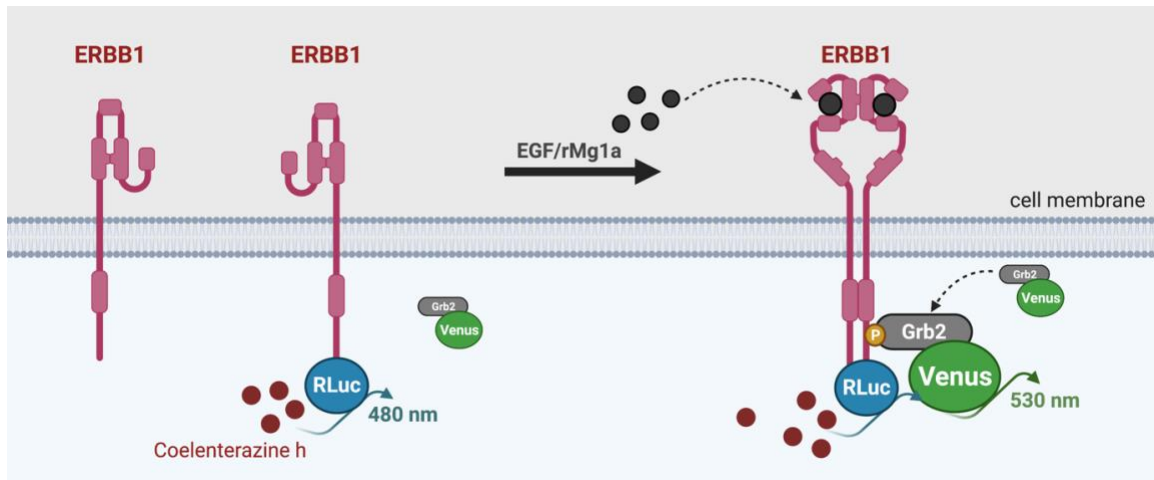


**Figure S4. Schematic of bioluminescence resonance energy transfer (BRET) assay.** ErbB1 receptors tagged with bioluminescent enzyme RLuc oxidize coelenterazine to release a blue photon at 480 nm. Upon receptor ligation, dimerization occurs, and subsequent auto-phosphorylation allows for recruitment of Grb2 with the attached acceptor fluorophore Venus. Upon close interaction (< 10 nm), energy transfer occurs between donor (RLuc) and acceptor (Venus), allowing for light production at 530 nm (instead of 480 nm).

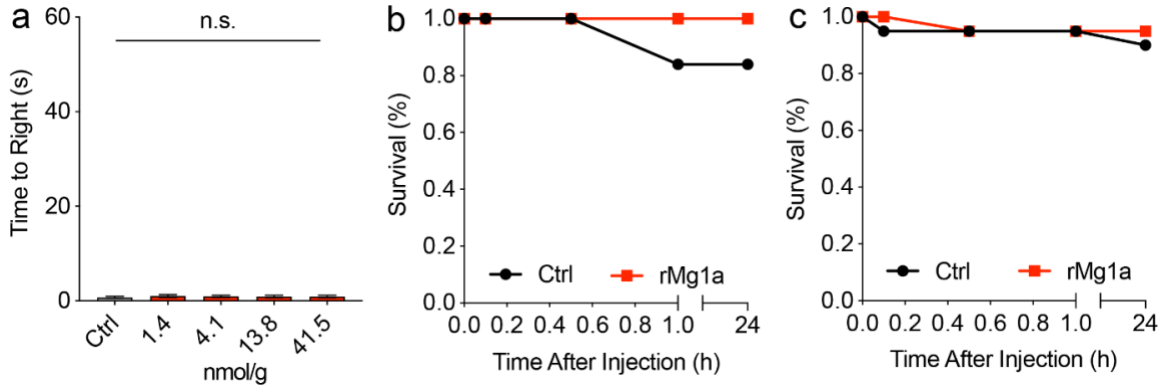


**Figure S5. rMg1a does not cause paralysis or death in insects.** (a) Intraabdominal injection of rMg1a (0.14 to 41 nmol/g) had no effect on the ability of crickets (*Acheta domesticus*) to right themselves ( $n = 5$  per group). (b) Intrathoracic injection of rMg1a (41 nmol/g) had no effect on the survival probability of adult sheep blowflies (*Lucilia cuprina*) ( $n = 15$  per group). (c) Intrathoracic injection of rMg1a (41 nmol/g) had no effect on the survival of *Drosophila melanogaster* ( $n = 15$  per group).

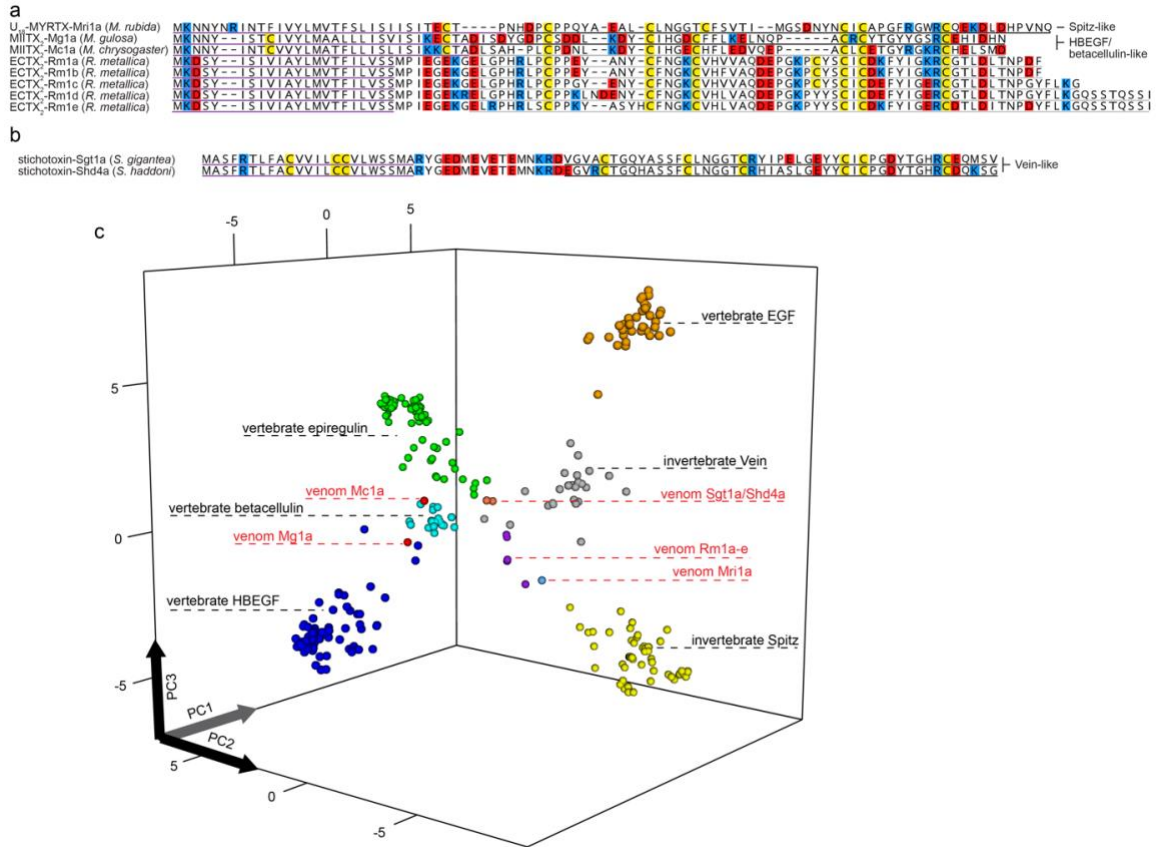


**Figure S6. EGF-like venom peptide families.** (a) Alignment of EGF-like peptides from ant venoms. Signal peptides, mature peptides and predicted mature peptides are underlined in purple, black and grey, respectively. Genes to which the mature peptides are analogous are indicated to the right of the panel. (b) Alignment of EGF-like peptides from sea anemone venoms: stichotoxin-Sgt1a (UniProt: Q76CA1) and stichotoxin-Shd4a (UniProt: B1B5J0). Labels are as in panel a. (c) Quantitative map of sequence space for the EGF-like peptide hormone superfamily and EGF-like venom peptides. Each point represents a non-redundant sequence. Points are coloured as follows: EGF, orange; HBEGF, blue; betacellulin, cyan; epiregulin, green; Spitz, yellow; Vein, grey; Mg1a and Mc1a, red; Rm1a-e, purple; Mri1a (UniProt: A0A6G9KJM3), light blue; Sgt1a (UniProt: Q76CA1) and Shd4a (UniProt: B1B5J0), pink.

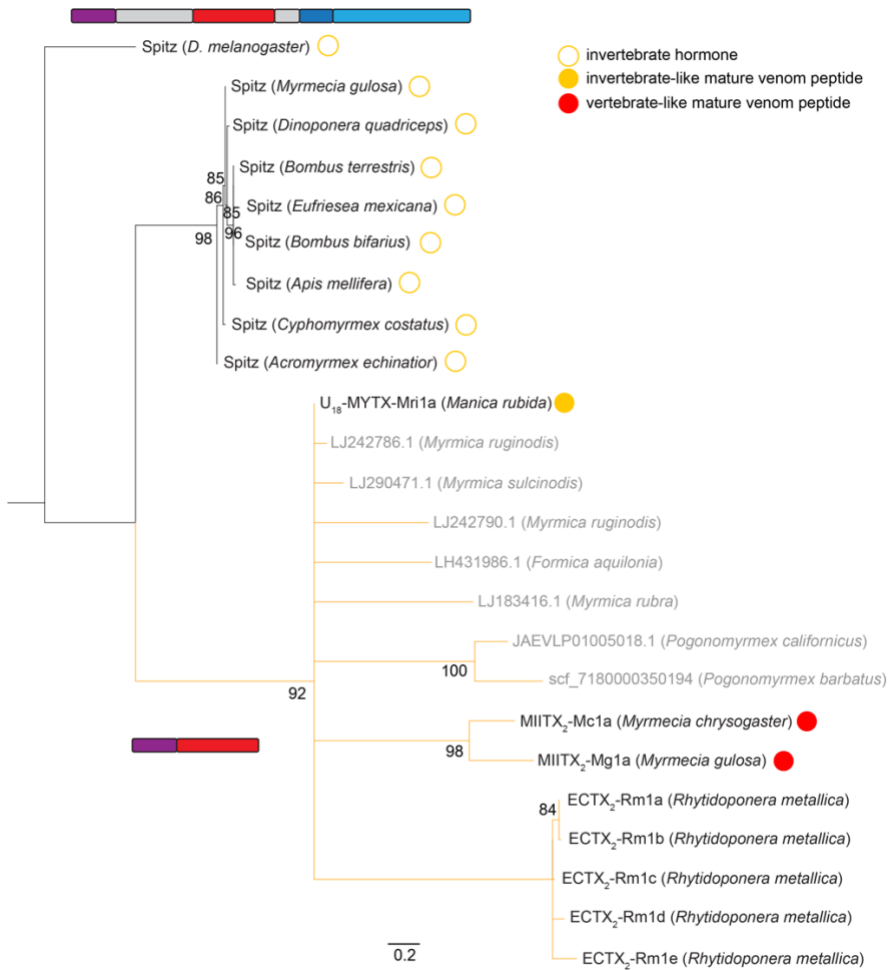


**Figure S7. Phylogenetic reconstruction of the ant venom EGF-like peptide toxins.** A maximum likelihood tree estimated from an alignment of the sequences of ant EGF toxin and toxin-like precursors and Spitz (truncated to signal and mature peptide only). *D. melanogaster* Spitz was used as the root. Branches representing endogenous Spitz sequences are colored black, while branches representing ant venom EGF-like peptide toxins are colored yellow. Branches representing, and names of, toxin-like sequences detected only in whole body transcriptomes or genomes are colored in grey. The prepropeptide architecture of endogenous Spitz and the ant venom EGF peptide toxins are indicated above and below each branch (color-coding is the same as in Fig. 1). Bootstrap proportions are indicated under each node.



**Table S1. Structural statistics for the NMR ensemble of rMg1a<sup>a</sup>**

PDB ID	7R6P
Experimental restraints	
Inter-proton distance restraints	
Total	671
Intra-residue ( $i = j$ )	177
Sequential ( $ i - j  = 1$ )	222
Medium range ( $1 <  i - j  < 5$ )	124
Long range ( $ i - j  \geq 5$ )	148
Disulfide bond restraints	9
Dihedral-angle restraints ( $\phi, \psi$ )	75
$\phi$ dihedral angle restraints	37
$\psi$ dihedral angle restraints	38
Mean number of restraints per residue	14.8
Violations of experimental restraints	0
RMSD to mean coordinate structure (Å)	
All backbone atoms	$0.71 \pm 0.12$
All heavy atoms	$1.07 \pm 0.09$
Backbone atoms (residues 3-48)	$0.43 \pm 0.10$
Heavy atoms (residues 3-48)	$0.90 \pm 0.11$
Stereochemical quality <sup>b</sup>	
Ramachandran plot statistics	
Residues in most favored Ramachandran region (%)	$95.3 \pm 2.3$
Disallowed regions [%]	$0.0 \pm 0.0$
Unfavorable sidechain rotamers [%]	$6.8 \pm 2.6$
Clashscore, all atoms <sup>c</sup>	$0.0 \pm 0.0$
Overall MolProbity score	$1.38 \pm 0.14$

<sup>a</sup>All statistics are given as mean  $\pm$  S.D.

<sup>b</sup>Stereochemical quality according to MolProbity (<http://helix.research.duhs.duke.edu>).

<sup>c</sup>Clashscore is defined as the number of steric overlaps  $>0.4$  Å per 1000 atoms.